IN VITRO TOXICITY AND INTRACELLULAR UPTAKE OF FLAME SYNTHESIZED IRON OXIDE NANOPARTICLES: AN ALTERNATIVE TO WET SYNTHESIS METHODS

Kivilcim Buyukhatipoglu, Drexel University, Philadelphia, PA
Tiffany Miller, Drexel University, Philadelphia, PA
Alisa Morss Clyne, Drexel University, Philadelphia, PA

Abstract

Superparamagnetic iron oxide nanoparticles, including magnetite (Fe_3O_4), are widely used in applications such as hyperthermic malignant cell treatment, magnetic resonance imaging, targeted drug delivery, tissue engineering, gene therapy, and cell membrane manipulation. In the current work, superparamagnetic iron oxide nanoparticles were produced using a flame synthesis method, which provides significant advantages over other material synthesis processes. Flame synthesis allows control of particle size, size distribution, phase and composition by altering flame operating conditions and is further capable of commercial production rates with minimal post-processing of the final product materials. This study focuses on the interaction of flame synthesized iron oxide nanoparticles with porcine aortic endothelial cells and compares the results to those obtained using commercially available iron oxide nanoparticles. The materials characteristics of the flame synthesized iron oxide nanoparticles, including morphology, elemental composition, particle size, and magnetic properties, were analyzed by electron microscopy (TEM, ESEM, EDS), and Raman Spectroscopy. The data verified production of a heterogenous mixture of hematite and magnetite nanoparticles, which exhibit superparamagnetic properties. Monodisperse iron oxide particles of 6-12 nm diameter and aggregated clusters of these 6-12nm nanoparticles have been synthesized. Nanoparticle biocompatibility was assessed by incubating flame synthesized and commercially available iron oxide nanoparticles with endothelial cells for 24 hours. Both Alamar blue and Live/Dead cell assays showed no significant toxicity difference between flame synthesized and commercially available nanoparticles. Cells exposed to both types of nanoparticles maintained membrane integrity, as indicated by minimal lactase dehydrogenase release. Endothelial cells imaged by ESEM and confirmed by EDS demonstrated that uncoated flame synthesized nanoparticles are ingested into cells in a similar manner to commercially available nanoparticles. These data suggest that flame synthesized iron oxide nanoparticles are comparable to commercially available nanoparticles for biological applications. Flame synthesis has the advantage of a relatively simple synthesis process with higher purity products and lower time and energy manufacturing costs. Future work will include functionalizing the nanoparticle surfaces for specific biological applications, including specific cell targeting and bioactive factor delivery.

Introduction

Recent developments in nanotechnology allow us to produce and functionalize nanoparticles for biomedical applications such as magnetic resonance imaging (MRI), hyperthermic treatment of malignant cells, targeted drug delivery, tissue engineering, and cell membrane manipulation [1-6]. Superparamagnetic nanoparticles, such as Fe_2O_3 and Fe_3O_4, are of particular interest for in vivo and in

vitro applications because they do not show any magnetic behavior after the magnetic field has been removed [7].

In this study, iron oxide nanoparticles were produced by gas phase combustion synthesis, also called flame synthesis. Flame synthesis can be simpler and more economical than other material synthesis techniques such as sol-gel processing, chemical vapor deposition and wet chemical deposition. In particular, flame synthesis produces a continuous high yield of pure material with controlled particle size, size distribution, phase, and composition in a single step with no subsequent post-processing (see Wooldridge and Pratsinis for details) [8-10]. Interaction of flame synthesized iron oxide nanoparticles with endothelial cells was investigated, since endothelial cells directly interact with nanoparticles in the bloodstream. Cytotoxicity results were compared to those obtained using commercially available iron oxide nanoparticles.

Methods

Nanoparticle Synthesis

A laboratory scale combustion synthesis and sampling system was developed for direct synthesis of iron oxide nanoparticles. The combustion synthesis system was composed of three main components: the burner consisting of three concentric tubes, which was used to create a high temperature synthesis environment; a liquid precursor delivery system; and two particle sampling mechanisms to obtain discrete and bulk material samples via thermophoretic deposition. A schematic of the combustion synthesis system is shown in Fig. 1.

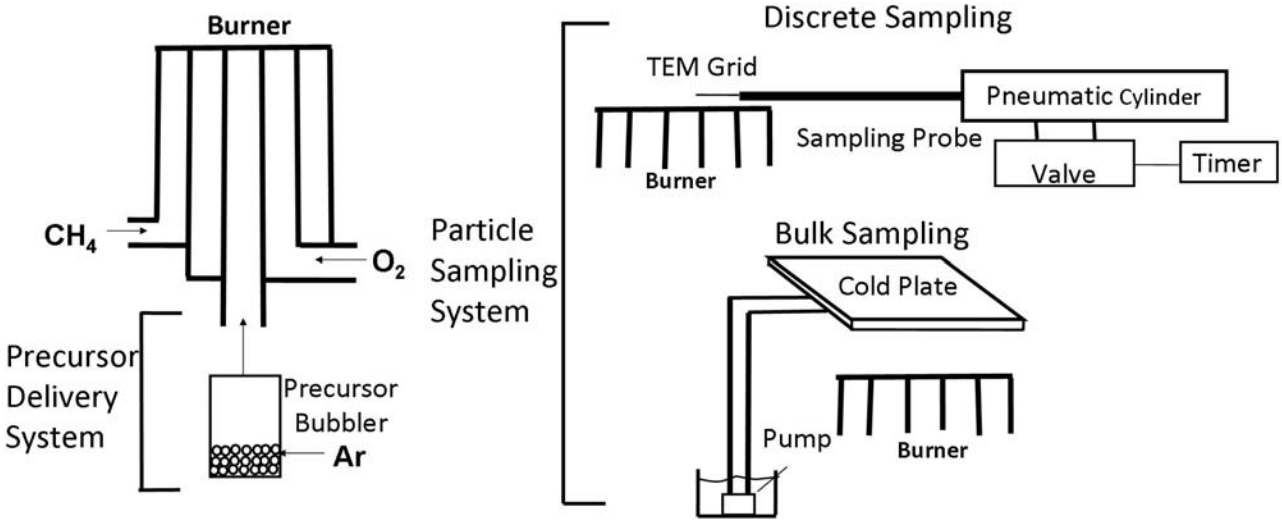

Figure 1: Schematic of combustion synthesis facility.

Nanoparticle Characterization

Nanoparticle morphology, elemental composition and size were analyzed by transmission electron microscopy (TEM; JEM-2000FX). The iron oxide nanoparticle elemental composition was analyzed using a Renishaw RM1000 VIS Raman microspectrometer with 633 nm excitation wavelength.

Cell Culture

Porcine aortic endothelial cells (PAEC) were maintained in low glucose Dulbecco's modified Eagle's medium (DMEM) supplemented with 5% fetal bovine serum, 1% penicillin-streptomycin, and

2% glutamine (Invitrogen). Culture media was changed every 48 hours and cells were used between passages 4 and 9. Confluent cells were incubated with media alone or media with 0.1 mg/ml iron oxide nanoparticles (flame synthesized or commercially available) for 24h. 10 ng/ml tumor necrosis factor-α (TNFα) was the positive control.

Scanning Electron Microscopy for Cell Morphology

Scanning electron microscopy (SEM) was used to visualize nanoparticle interaction with cells. PAEC were seeded on 8mm sterile glass coverslips and incubated with nanoparticles as previously described. Cells were fixed in 3% glutaraldehyde (EMS) at room temperature for 20 minutes, rinsed three times with phosphate buffered saline (PBS), and dehydrated in graded ethanol (Pharmco). Ethanol was then replaced with hexamethyldisilazane (HMDS; EMS), and samples were dried by overnight HMDS evaporation in a chemical fume hood. Samples were desiccated under vacuum, sputter coated with 0.75nm thick Pt/Pd layer to increase conductivity, and viewed under a Zeiss Supra 50VP SEM.

Nanoparticle Cytotoxicity

Alamar blue was used to measure cell proliferation and metabolic activity using an oxidation-reduction indicator. After 24 hours of cell nanoparticle exposure, 100µl of media from each condition was transferred into a 96 well flat-bottomed black assay plate. 10µl of Alamar Blue (AbD Serotec) was added to each well, and the well plate was incubated for 4h at 37°C. Fluorescence was measured at 535/590 nm in a GENios microplate reader.

The CytoTox-ONE Homogenous membrane integrity assay kit (Promega) measures release of lactate dehydrogenase (LDH) from cells with damaged membranes. 100 µl of media from PAEC incubated with nanoparticles for 24 hours was transferred into a 96 well flat-bottomed black plate. 100 µl of CytoTox-ONE reagent was added to each well, after which the plate was incubated at room temperature for 10 minutes protected from light. Fluorescence was measured at 560/590 nm in a GENios microplate reader.

The Live-Dead Assay (Molecular Probes) quantifies live and dead cells by measuring intracellular esterase activity (Calcein AM, green) and plasma membrane integrity (ethidium homodimer-1, red). PAEC seeded on sterile 13-mm round glass coverslips were incubated with nanoparticles for 24 h, washed with PBS, and treated with 150µl of 2µM calcein AM and 4 µM of ethidium homodimer-1 as per manufacturer instructions. Cells were incubated at room temperature for 45 minutes and imaged in an Olympus IX81 inverted fluorescent microscope.

Results and Discussion

Two different size modes of iron oxide nanoparticles were synthesized using the flame synthesis method. Iron pentacarbonyl, $Fe(CO)_5$, was used as the liquid precursor and delivered to the central annulus of the reactor as saturated vapor entrained in Argon gas. All synthesis conditions were conducted under oxygen rich conditions with low equivalence ratios to minimize unwanted carbon contamination in the synthesized nanoparticles. An inverse diffusion flame configuration, with O_2 in the second annulus (flowrate: 3546 ml/min) and CH_4 in the third annulus (flowrate: 494ml/min), resulted in a high concentration of magnetite formation as verified by Raman spectroscopy. Representative TEM images of flame synthesized 6-12 nm iron oxide nanoparticles and small aggregated clusters of them collected at 5cm above the burner exit are shown in Fig. 2a. Raman spectroscopy of synthesized nanoparticles (Fig. 2b) showed a heterogeneous mixture of two common

forms of iron oxide, hematite and magnetite, in the nanoparticles. The intense peak observed at 1320 cm^{-1} is assigned to a two-magnon scattering which arises from interaction of magnons created on antiparallel close spin sites [11].

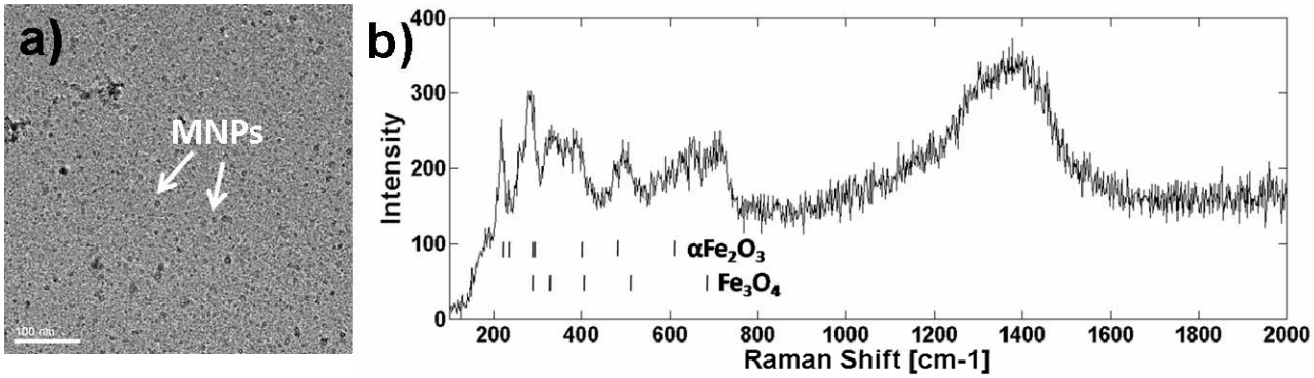

Figure 2: TEM images show monodispersed and aggregated clusters of 6-12 nm diameter iron oxide nanoparticles (a). Raman spectrum of flame synthesized iron oxide nanoparticles show magnetite, Fe_3O_4, and hematite, αFe_2O_3 content of the nanoparticles produced (b).

Endothelial cells remained attached and spread after 24 hours of exposure to 0.5 mg/ml nanoparticle solution. When incubated with nanoparticles (Fig. b, c), endothelial cells were less spread, more rounded, and appeared to have lost their typical cobblestone morphology, however no change in cell adhesion and total attached cell number was observed (Fig. 3 d)

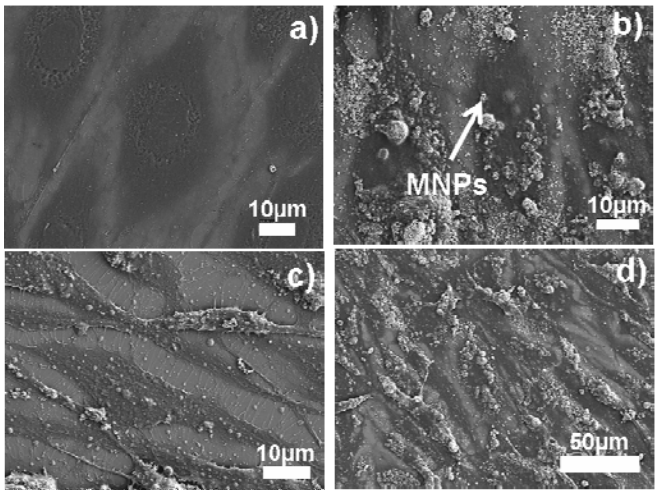

Figure 3: SEM images show that Individual cell spread less when incubated with nanoparticles (b, c). However there was no observed change in attached cell number and adhesion (d).

Flame synthesized superparamagnetic nanoparticles demonstrated low cytotoxicity comparable to commercially available nanoparticles. Endothelial cell viability, as measured by Alamar blue, did not change with nanoparticle exposure or with synthesis method (Fig. 4a). Endothelial cells demonstrated a slight loss of membrane integrity with purchased nanoparticles, as measured by LDH release, (Fig. 4b). However, no statistically significant changes in cell membrane integrity were observed in cells exposed to synthesized nanoparticles.

Endothelial cell viability with both synthesized and purchased nanoparticles was confirmed using a Live/Dead Cell Viability assay. When dead cell number was quantified using a microplate reader, cells exposed to both purchased and synthesized iron oxide nanoparticles showed slightly increased cell death over control cells (Fig. 4c). However, there was no statistically significant change in cell death for the two types of nanoparticles. Fluorescent images of representative cell regions showed no observable difference in live and dead cell density (Fig. 4 d, e, f).

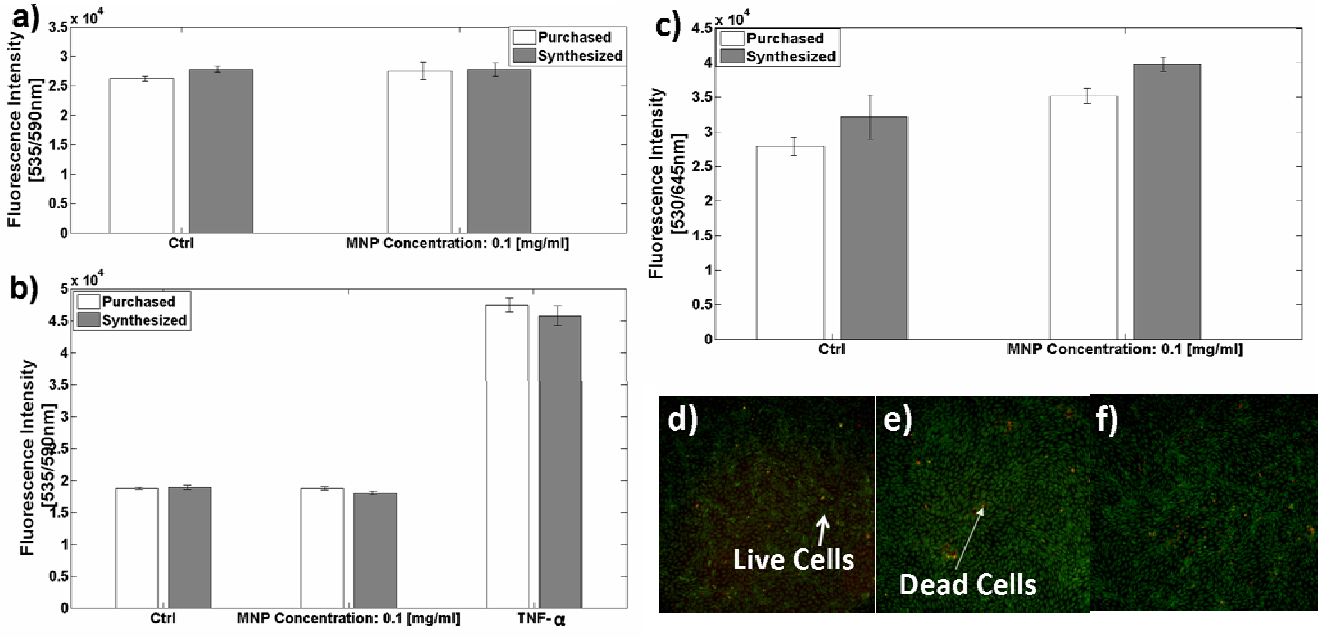

Figure 4: (a) Alamar blue, (b) LDH, (c) Live/Dead assays showed no significant difference in cytotoxicity between flame synthesized and commercially available nanoparticles. Live-Dead cell numbers are also compared with the data obtained from microplate reader by counting the cells at the fluorescent images: control cells (d), cells loaded with 0.1 mg/ml of purchased nanoparticles (e), cells loaded with 0.1mg/ml of synthesized nanoparticles (f).

Conclusions

Iron oxide nanoparticles were synthesized using flame synthesis, which has the advantage of being a relatively simple synthesis process with higher purity products and lower time and energy manufacturing costs. Cellular uptake and cytotoxicity studies suggest that flame synthesized iron oxide nanoparticles are comparable to commercially available nanoparticles for biological applications. Future work will include functionalizing the nanoparticle surface for specific biological applications, including cell targeting and bioactive factor delivery.

References

1. Halavaara, J. et al. (2002), "Efficacy of sequential use of superparamagnetic iron oxide and gadolinium in liver MR imaging," *Acta Radiol.*, 43(2): p. 180-5.
2. Bonnemain, B. (1998), "Superparamagnetic agents in magnetic resonance imaging: physicochemical characteristics and clinical applications. A review," *J Drug Target*, 6(3): p. 167-74.

3. Mitsumori, M., et al. (1996), Targeted hyperthermia using dextran magnetite complex: A new treatment modality for liver tumors. Hepato-Gastroenterology,"43(12): p. 1431-1437.
4. Scherer, F., et al. (2002), "Magnetofection: enhancing and targeting gene delivery by magnetic force in vitro and in vivo. Gene Therapy," 9(2): p. 102-109.
5. Dobson, J. (2006), "Gene therapy progress and prospects: magnetic nanoparticle-based gene delivery. Gene Therapy," 13(4): p. 283-287.
6. Gupta, A.K. and A.S.G. Curtis (2004), "Surface modified superparamagnetic nanoparticles for drug delivery: Interaction studies with human fibroblasts in culture," Journal of Materials Science-Materials in Medicine, 15(4): p. 493-496.
7. Gupta, A.K. and M. Gupta (2005), "Synthesis and surface engineering of iron oxide nanoparticles for biomedical applications," Biomaterials, 26(18): p. 3995-4021.
8. Wooldridge, M.S. (1998), "Gas-phase combustion synthesis of particles," Progress in Energy and Combustion Science, 24(1): p. 63-87.
9. Pratsinis, S.E. (1998), "Flame aerosol synthesis of ceramic powders," Progress in Energy and Combustion Science, 24(3): p. 197-219.
10. Kammler, H.K., L. Madler, and S.E. Pratsinis (2001), "Flame synthesis of nanoparticles," Chemical Engineering & Technology, 24(6): p. 583-596.
11. deFaria, D.L.A., S.V. Silva, and M.T. deOliveira (1997), "Raman microspectroscopy of some iron oxides and oxyhydroxides, " Journal of Raman Spectroscopy, 28(11): p. 873-878.